Volume Segmentation with Gray-Level and Spatial Correlation-Based Entropic Thresholding, Contour Detection and Contour Extraction from Tomographic Image Data

Mariam Ghochani, Arlette R.C. Baljon, Terrence G. Frey
and Carlos Bazan

August 2010

Computational Science &
Engineering Faculty and Students
Research Articles

Database Powered by the
Computational Science Research Center
Computing Group

COMPUTATIONAL SCIENCE & ENGINEERING

SAN DIEGO STATE UNIVERSITY

Computational Science Research Center
College of Sciences
5500 Campanile Drive
San Diego, CA 92182-1245
(619) 594-3430

Volume Segmentation with Gray-Level and Spatial Correlation-Based Entropic Thresholding, Contour Detection and Contour Extraction from Tomographic Image Data

Mariam Ghochani[1,2,3], Arlette R.C. Baljon[1], Terrence G. Frey[2], Carlos Bazan[3]
[1]Department of Physics, San Diego State University, San Diego California 92182
[2]Department of Biology, San Diego State University, San Diego California 92182
[3]Computational Science Center, San Diego State University, San Diego California 92182
*Corresponding author: Mariam Ghochani, mariamghochani@gmail.com

Abstract: With the advancements in optical systems and tomographic reconstruction techniques, researchers are able to produce three-dimensional image data sets at ultrastructure resolutions of electron microscope. To visualize such data sets in order to conclude structural information, three-dimensional modeling techniques are being developed in order make contours of the detected structures in the volume image data. Such contours can then be rendered into surfaces to create volume models. Manual volume segmentation allows researchers to manually trace and label contours of the structures of interest. However, this is a time consuming process which can be done more efficiently with development of techniques for automatic or semi-automatic contour extraction methods. This paper outlines a model that incorporates nonlinear diffusion across the volume to eliminate noise that corrupts the imaged biological structures. An entropic thresholding based on gray-level and spatial correlation across the data volume is then incorporated into this model. It follows with an edge detection model and contour extraction to label extracted connected contours. Such contours can be exported to a volume rendering environment to produce volume models in an automatic or semi-automatic manner.

Keywords: tomographic data, nonlinear diffusion, local entropic thresholding, Canny contour detection, contour extraction.

1. Introduction

Ultrastructure studies in biophysics and structural biology is advanced as a result of the amount and diversity of information that can be obtained from three-dimensional (3D) image data sets from electron microscope. Advancements in electron microscopes, sample preparation and computational techniques has played a major part in improvement of the finalized 3D image data sets. Currently there are high demands for computation methods that allow visualization and analysis of such complex image data sets. Convenient visualization and display of the 3D image data set result in better understanding the structure under study. The 3D image data is provided from a volume of material, in which each voxel has a single intensity value. Examples of these data are tomographic reconstructions that provide serial section images from the volume of the material from an electron microscope and optical sections from a light microscope. The programs such as IMOD (http://bio3d.colorado.edu/imod/), XVOXTRACE and JINX (http://ncmir.ucsd.edu/) that are used for analysis of 3D image data, allow users to manually create data sets (manual tracing/labeling) that contain list of scattered points, list of contours describing a surface, or list of connected line segments, which can then be used for volume rendering [6]. The output of volume rendering process is a 3D Model based on stack of membrane contours that can be rotated and viewed at different angles. In order to create such data sets automatically using edge detection methods, edge-lists of closed edges that are well-detected and well-localized by a detector (filter) should become available from the 3D image data. Well-detection is equivalent to having no missing edges and no responses to non-edges. Well-localization means that the distance between the detected edge pixels and the actual edge is at a minimum. Edges identified by edge detection methods are often disconnected so it should be combined by other techniques as to have closed edges where possible, to be labeled in the edge-list prior to volume rendering. Then one way to provide the data that is needed for volume rendering is to develop an approach where closed edges with such criteria are computationally detected along the volume of the 3D image data set. Then the edge-lists containing the coordinates of sequential edge pixels are stored, one list for each edge contour. They can then be modified to group lists of contours describing a certain surface together. It would then be possible to make such edge-lists compatible and exportable to a surface rendering program such as IMOD or Jinx for subsequent rendering to visualize the 3D model.

Various methods are developed for 3D image segmentation. Through 3D image segmentation, one can partition the 3D data into segments, which allow label assignment to every pixel in the data. The labels can be assigned so that pixels with the same label share certain visual characteristics. Image segmentation methods can be grouped into gray-value based, region based and shape based categories. There are other methods such as Fuzzy connectedness and Watershed algorithms that do not fall cleanly into these categories [10]. Models of 3D entropic thresholding to segment the volume to object and background while closing the inter-ruptured structures and improving segmentation of connected edges, and volume segmentation using edge detection techniques by hysteresis thresholding to segment connected edges that are modified and used in this study fall into the category of gray-value based 3D image segmentation.

This paper is organized as follows: Section 2 briefly describes methods of preparing the 3D image data set. Section 3 presents the models of 3D nonlinear diffusion and bilateral filtering combined (implemented in terms of [9], [4], [1]), entropic threshold selection method based on 3D gray-level spatial correlation (GLSC) histogram (implemented in terms of [11]) and Canny edge detection model with use of hysteresis thresholding applied to 3D image data set (implemented in terms of [3]). Section 4 includes the numerical experiment (proposed model) and numerical results. The paper ends with a summary and discussion in section 5. The nonlinear diffusion method and entropic threshold selection method are applied across the volume while canny edge detection model and contour labeling are done on each 3D serial section image. This is done so that the contours based on the features of interest from each image section can be selected.

2. Image Acquisition

The tomographic 3D image data set was calculated from series of tilted views of volume of material from an electron microscope by use of the R-weighted back projection algorithm [5]. IMOD software package is used to compute the tomogram by the R-weighted back projection algorithm. Prior to application of this algorithm, the tilt series was first aligned by creating a list of fiducial points. The minimization approach described by Luther el al. is used through the program TILTALIGN as part of the IMOD tomography package to solve for shifts, rotations and size changes needed to align the views [8]. Five sequential serial section images spanning a volume of ~ 15 nm are used for the numerical experiment in this study.

3. Related Models

In this section an overview of the related models is presented to serve as a background to the model proposed in this study. The proposed modifications to these related models are described which are then further elaborated on in Section 4.

3.1 Nonlinear Diffusion Model

Tomographic 3D image data from biological material usually contain large amount of noise that can corrupt the structural patterns. Nonlinear diffusion is a very powerful technique to reduce noise while enhancing the structural features. The model that is used in this study to enhance structures by denoising is an incorporation of Perona and Malik model where regularization is proposed directly into the PDE to avoid the dependence on the numerical schemes based on the formulation due to Catt´e, Lions, Morel and Coll with the refinement proposed by Bazan and Blomgren [9], [4], [1]. The model is written as

$$\begin{aligned} &\partial_t u - \nabla \cdot \left(g\left(\|\nabla u_{BF}\|^2 \right) \nabla u \right) = 0 \\ &\partial_{\vec{n}} u = 0, \quad u(\vec{x},0) = u_0(\vec{x}) \end{aligned} \tag{1}$$

Perona and Malik nonlinear diffusion model avoids the blurring of edges and other localization problems presented by linear diffusion models by reducing the diffusivity in places with higher likelihood of being edges. The likelihood is measured by a function of the local gradient $\|\nabla u\|$ in terms of the current image and $\partial_{\vec{n}} gu = 0$ is the Neumann boundary conditions. The diffusivity of Perona and Malik model is such that $g(\|\nabla u\|)^2 \to 0$ when $\|\nabla u\| \to \infty$ and $g(\|\nabla u\|)^2 \to 1$ when $\|\nabla u\| \to 0$ as

$$g\left(\|\nabla u\|^2\right) = \frac{1}{1 + \|\nabla u\|^2 / \lambda^2}, \quad \lambda > 0 \qquad (2)$$

In the attempt of introducing the regularization directly into the PDE, Catt´e, Lions, Morel and Coll model proposed replacing the Perona and Malik diffusivity by $g(\|\nabla u_\sigma\|)^2$ where likelihood of being edges is measured in terms of the local gradient of the current image u_σ; that is the smooth version of the current image by a Gaussian kernel of variance σ^2. With this Gaussian filtering, the diffusivity term allows detection of the locations of the main edges to prevent excessive diffusion while the small noise fluctuations will not be detected as edges hence diffused away since they will be smooth. Incorporating the Bazan and Blomgren refinement for the gradient estimator, a bilateral filter in place of the Gaussian kernel is applied. The main purpose of the diffusivity term is to provide selective smoothing by precisely locating the position of the main edges and inhibiting diffusion at those locations. With the bilateral filtering, a spatial Gaussian and a range Gaussian are applied to smooth the image at every location where they decrease the influence of distant pixels and decrease the influence of the pixels with intensity values that are very different respectively. Then by design the bilateral filter provides strict preservation of the edges without artificially enhancing them hence improving the selectivity of the diffusivity term when

$$g\left(\|\nabla u_{BF}\|^2\right) = \frac{1}{1 + \|\nabla u_{BF}\|^2 / \lambda^2}, \quad \lambda > 0, \qquad (3)$$

For this study Canny's noise estimator is used to determine λ as the 90 percentile of the magnitude of the gradient for the edges in terms of the original image smooth by the bilateral filter; since the local gradient for the diffusivity term is set in terms of the smooth version of the current image by a bilateral filter.

Bazan et al. has used a method of anisotropic nonlinear diffusion for tomographic data where it not only account for modulus of the edge detector, but also its directional information; hence by choosing appropriate eigenvalues, one can allow smoothing parallel to the edges and avoid doing so across them [2]. For this study, this approach is not used for denoising since entropic thresholding in terms of the 3D gray-level spatial correlation that is introduced in the next section can to some extend improve smoothing parallel to the edges; due to its spatial correlation dependence.

The nonlinear diffusion in this study is applied throughout the 3D image data where the gradient and divergence operator are computed not only along the x and y directions in each serial section image but also across the serial section images in the z direction. This allows modulation of diffusivity in terms of patterns across the serial images as well as each serial section image.

3.2 Entropic Threshold Selection from GLSC

When using edge detection as part of contour extraction, edges are often disconnected. Canny edge detection model proposes hysteresis thresholding in an attempt to segment connected edges but pre-segmentation and pre-thresholding is not incorporated. In biological 3D image data, due to characteristics of the imaged material as well as some effects from tomographic computation method such as wedge effect (missing some high frequency details in the 3D image data), there are many inter-ruptured structures. In this case use of a thresholding scheme in terms of the spatial as well as gray-level correlation of the voxels can help to either close the inter-ruptured structures or eliminate them from the object depending on if they are included as part of the object or the background when threshold is chosen.

The approach in thresholding schemes is to select a value ϕ, and sets foreground voxels, accordingly,

$$\min_{x,y,z}\left(u(x,y,z)\right) \le \phi \le \max_{x,y,z}\left(u(x,y,z)\right)$$
$$v(x,y,z) = \begin{cases} 255 & \text{if } u(x,y,z) \ge \phi \\ 0 & \text{else} \end{cases} \qquad (4)$$

Based on different model assumption, there are different solutions to the above binarization algorithm. When there is low signal to noise ratio or when the object and background gray value intensities are not constant throughout the volume, even with an optimal selection of ϕ the results will not be satisfactory. For the case study at hand, the intensity histogram equalization is performed across the volume using the IMOD package. The expectation is that with the use of the nonlinear diffusion model as described before the influence of the noise is removed optimally; hence increasing the signal to noise ratio.

One approach to determine an optimal threshold value is through entropic maximization as in concept in information theory. In various models of entropic methods by Pun [1981], Kapur [1985], Renyi's entropy [1997] and Tsallis's entropy [2004], the image spatial correlation is not considered. In Abutaleb's model, the gray value of the pixels and the local gray-value of the pixels are used to set up a 2D histogram for entropic thresholding approach [11]. This approach bears resemblance to using "shading correction" when the mean intensity value within a window around each pixel in subtracted from each pixel as part of local thresholding approach in 2D image processing [10].

For this study, the image local property is incorporated in thresholding based on the GLSC histogram proposed by Xiao, Cao and Zhang. The refinement is done as part of segmentation of 3D image data in computing the GLSC histogram across the image volume. The GLSC histogram takes into account the image local property by using the gray value of the pixels and their similarity with neighboring pixels in gray value.

The 3D GLSC histogram is computed as follows. With $u(x,y,z)$ being the gray value of the voxel at (x,y,z) in the 3D image data, then $m(x,y,z)$ is defined as the number of neighboring voxels that their gray-level is close to the voxel located at (x,y,z) (neighbor voxels). For this study the gray-levels across the volume are between [0,255], the corresponding neighboring voxels are chosen from a $3\times3\times3$ volume and when the intensity of the voxels are within 4 gray-levels, then their gray-levels are considered close to each other such that,

$$m(x,y,z)= \sum_{i=-1}^{i=1}\sum_{j=-1}^{j=1}\sum_{k=-1}^{k=1}\varsigma\big(u(x+i,y+j,z+k)-u(x,y,z)\le 4\big) \quad (5)$$

where

$$\varsigma\big(u(x+i,y+j,z+k)-u(x,y,z)\le 4\big)= \begin{cases}1 & u(x+i,y+j,z+k)-u(x,y,z)\le 4\\ 0 & u(x+i,y+j,z+k)-u(x,y,z)> 4\end{cases} \quad (6)$$

Then the normalized probability of a voxel with gray-level k and m neighbor voxels $(h(k,m))$ can be computed.

At a threshold t segmenting the object from the background, the entropies of the object and that of the background are

$$H_A(t)=-\sum_{k=0}^{t}\sum_{m=0}^{27}\frac{h(k,m)}{P_A(t)}\ln\left(\frac{h(k,m)}{P_A(t)}\right)Weight(m) \quad (7)$$

and

$$H_B(t)=-\sum_{k=t+1}^{255}\sum_{m=0}^{27}\frac{h(k,m)}{P_B(t)}\ln\left(\frac{h(k,m)}{P_B(t)}\right)Weight(m) \quad (8)$$

respectively, where $weight(m)=\frac{1+\exp(-m)}{1-\exp(-m)}$, $P_A(t)=\sum_{k=0}^{t}\sum_{m=0}^{27}p(k,m)$ and $P_B(t)=\sum_{k=t+1}^{255}\sum_{m=0}^{27}p(k,m)$.

As the grey-level of the background is more homogeneous than that of the edges and the noise and since it has less information quantity, different weights are assigned in terms of the number of neighbor voxels in calculation of entropy such that as the number of neighbor voxels increases the weight decreases (similar to the weights proposed by Xiao, Cao and Zhang). Then the optimal threshold t^* can be obtained by maximizing the sum of the background and object entropies.

3.3 Canny Edge Detection Model

Kovesi has argued that most of the edge detection methods has focused on detection of the step edges and that the research on detection of step edges has resulted in edge detectors that fail to detect and correctly localize valid features that can be recognized by human eyes as part of manual contour extractions for volume rendering of 3D models [7]. Then in order to use an edge detector that can detect close edge contours of the various features that have been manually traced/labeled in 3D modeling programs such as IMOD (refer to the list by Kremer that was given in Section 1), one should use an edge detector that can detect and localize many edge type features that are somewhere between a step and a line including detection of lines, peaks, roofs and bars. The line and step edge detection by Canny [3] is an exception that allows detection of edge features other than step edges.

Canny has shown that with $H_G = \int_{-w}^{w} G(-x) f(x) dx$ being the response of a detector $f(x)$ to an edge in the finite impulse response bounded by $[-w, w]$ in 1D and $H_n = n_0 \left[\int_{-w}^{w} f^2(x) dx \right]^{1/2}$ being the root-mean-square response to the 1D noise $n(x)$, then the problem of well-detection of edges with a well-localization constraint is an optimization problem to find $f(x)$ that maximizes

$$\frac{\left| \int_{-w}^{w} G(-x) f(x) dx \right|}{n_0 \sqrt{\int_{-w}^{w} f^2(x) dx}} \frac{\left| \int_{-w}^{w} G'(-x) f'(x) dx \right|}{n_0 \sqrt{\int_{-w}^{w} f'^2(x) dx}} \tag{9}$$

This equation will be modified when including other constraints such as multiple response constraint. Canny has shown that with the detector being approximated as the first derivative of Gaussian operator, the final optimization can be achieved and this work can be extended to 2D space. So then the Canny method finds edges by looking for the local maxima of the gradient that is calculated using the first derivative of Gaussian operator. The response of this detector is compared to the response from boxed detectors and Laplacian of Gaussian operator suggested by Marr and Hildreth 1980 model in 1D and in 2D showing that the canny edge detector has a better impulse response that the boxed detector in 1D and performs a better localization and detection than finding the zero-crossing of Laplacian of Gaussian in 2D. In 2D boxed detectors are comparable to Sobel and Prewitt edge detectors and log filter searches for zero-crossing after the Laplacian of Gaussian is used to find the gradient to detect edges.

With Canny edge detection to be implemented for this study one should find the direction of the gradient to be in one of 0 deg, 45 deg, 90 deg or 135 deg intervals to describe one of the four possible directions when describing the surrounding pixels to a central pixel. Then by determining the directions of the gradient, non-maximum suppression is applied to trace along the edge in the gradient direction and suppress any pixels values (sets it equal to 0) that is not considered to be an edge resulting in a thin line in the output image. For extending this work to 3D image data, one can compute the direction of the gradient in terms of the axis across the serial image sections to suppress the non-edge voxels across the serial section images. Another specific approach in Canny edge detector is the use of hysteresis thresholding to eliminate streaking. Streaking is having disconnected edge contours since the operator output in the edge strength map fluctuates above and below the threshold when performing non-maximum suppression as a result of noise. With double thresholding in Canny detector implementation any voxel that has a value greater than the upper threshold is presumed to be an edge voxel and is marked as such. Any voxel connected to this edge voxel that has a value greater than the lower threshold is selected as an edge voxel as well resulting in connected contours when possible. However when this method is combined with a pre-thresholding that takes into account the spatial correlation of the voxels as well as their gray-level correlation (local thresholding) as described in Section 3.2, the effect of many inter-ruptured structures in the 3D image data of the biological material can be minimized in creating false edge connections or missing a small number of edge connections due to non-maximum suppresion.

4. Numerical Experiment and Numerical Results

Nonlinear diffusion combined with bilateral filtering of the local (current) image for finding and updating a selective diffusivity term, is performed on the serial image sections in the 3D image data; this is the step for initial denoising prior to finding the 3D GLSC for entropic thresholding. The nonlinear diffusion is implemented across the image volume incorporating the gradient and diffusion in all three $[x, y, z]$ directions. Second order gradient is computed on the boundaries. A single $\lambda = 0.239$ parameter is obtained from Canny noise estimator from the gradient of the filtered initial image. The initial image in filtered with a bilateral filter with the same parameters as the ones used for filtering each local (current) image when updating the diffusivity term. This approach results in selection of a smaller λ parameter leading to smaller diffusion at the well-preserved but not artificially enhanced edges through bilateral filter. The $\sigma_s = 3$ and $\sigma_r = 0.03$ parameters for bilateral filter are chosen to obtain the desired amount of low-pass filtering and combination of filtered values; for this study Tomasi and Manduchi (1998) implementation of bilateral filter for gray and color images in used. Time-step for implementation is set to $\tau = 10^{-2}$ and the determination of diffusion stopping criterion is similar to stopping criterion proposed by Bazan and Blomgren (2007) by finding the iteration that corresponds to the inflection point in the plot of correlation between the noisy serial section image and the improved ones. Figure 1 shows the 5 serial image sections with equalized intensity values across the volume and the result of denoising with this nonlinear diffusion model.

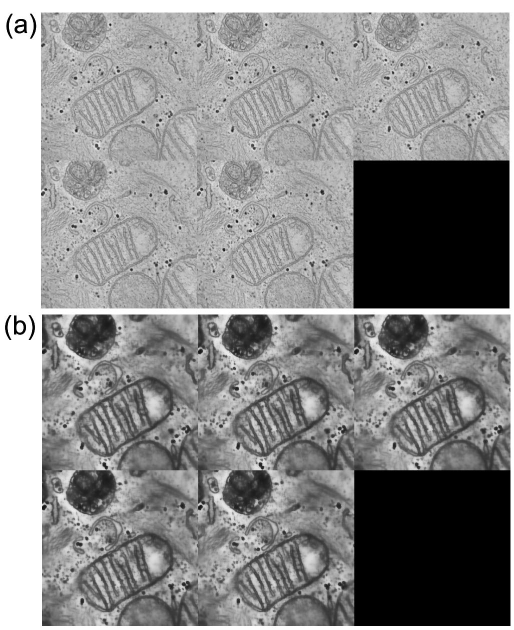

Figure 1. Serial sections before (a) and after (b) denoising.

Figure 2 shows the structure of the 2D probability distribution matrix of from 3D GLSC across 3D image data. Mesh of the matrix of normalized probabilities gives the 2D histogram based on 3D GLSC (Figure 3). Figure 2 also shows how the terms for entropy calculations at different thresholds (t) are obtained for this implementation where optimal threshold (t^*) is selected where the sum of the entropies from background and object is at the maximum. The optimum threshold $t^* = 111$ is found from this entropic thresholding in terms of 3D GLSC. Figure 4 shows the result when segmenting the volume at this threshold.

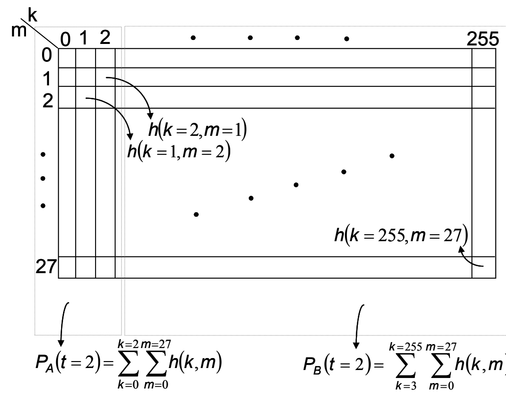

Figure 2. Probability distribution 2D matrix in terms of gray-level and number of neighbor voxels as part of the 3D GLSC implementation for entropic calculations at different thresholds.

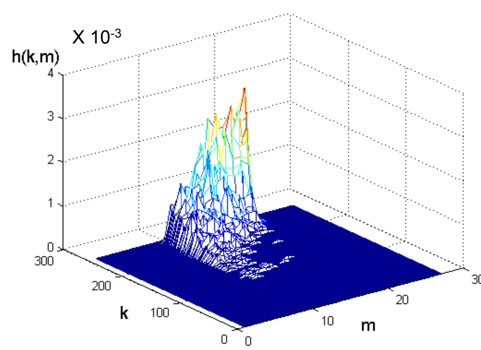

Figure 3. Two-dimensional histogram from 3D GLSC across the 3D image data.

The implementation of Canny edge detector with non-maximum suppression and hysteresis thresholding is next applied to the pre-segmented result from of Figure 4. The hysteresis thresholds are set at 0.1 and 0.2. Gradient detection with first derivative of Gaussian operator, non-maximum suppression and hysteresis thresholding to connect edge contours are done in two dimensions across each serial image section.

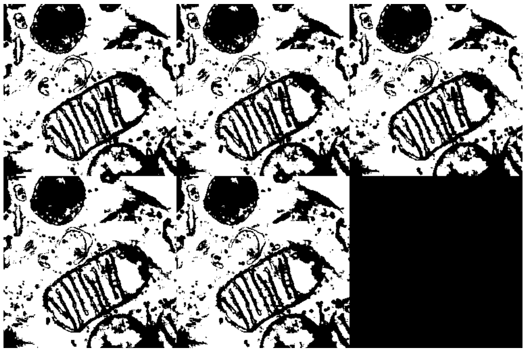

Figure 4. 3D image data segmentation with entropic thresholding based on 3D GLSC.

There must be a refinement when these models are implemented in three dimensions across the image volume. However since the nonlinear diffusion and entropic thresholding for pre-segmentation were performed across the image volume, a good portion of data association across the serial image sections is preserved. The connected and well-localized edges that are detected in this manner across the volume can be observed in Figure 5.

Figure 5. Connected and well-localized edge contours that are detected using Canny edge detector when pre-segmentation is performed.

Figure 6 shows the result from using Canny detector without the suggested pre-segmentation with entropic thresholding. By comparing Figure 5 and Figure 6, it can be observed that using this pre-segmentation model helps in connecting many of the edge contours while eliminating some of the false edge contour connections of the characteristic inter-ruptured structures in the 3D image data from biological material as they are partly eliminated as background.

The result in Figure 5 is used for labeling closed edge contours. In Figure 7 these labeled contours are shown with different colors plotted on original serial image sections from tomographic volume. For labeling contours, Kovesi (2001-2007) implementation of edge-linking and edge-labeling is used to link edge pixels together into list of sequential edge points; one list for each edge contour where it starts/stops at an ending or a junction with another edge-list (http://www.csse.uwa.edu.au/~pk/Research/MatlabFns/). For the case at hand the interest was in segmentation and contour extraction from the mitochondrial structure in the tomographic reconstruction. This structure can be isolated with adding empty 3D masks to the 3D image data where needed. Then when labeling the closed contours is performed we will only have edge-lists of the contours of interest.

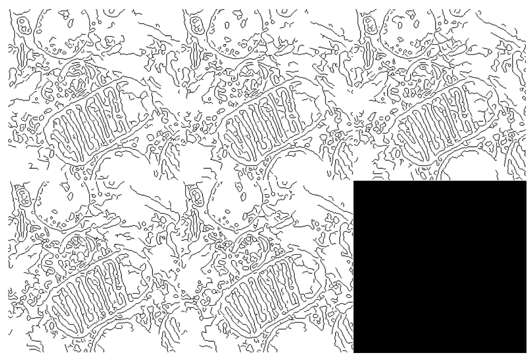

Figure 6. Edge contours from Canny edge detector without pre-segmentation.

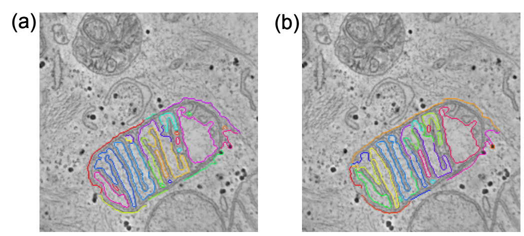

Figure 7. Labeled contours are extracted and shown on the original serial image sections ((a) and (b)) from tomographic volume.

Since the edge-lists are matrices of data containing the coordinates of sequential edge pixels they can be combined as a major extracted contour for surface rendering purposes. For example, the lists of the labeled closed contours inside the mitochondrial structure (inner membrane structures) can be combined as one list for extracted inner membrane contour; while the lists of the labeled contours outlining the mitochondrial structure can be combined as one list for extracted outer membrane contour from each serial image section across the 3D image data. When these lists are made compatible and exportable to volume rendering software such as IMOD or JINX and rendered, then this automatic volume segmentation model can be applied in place of manual contour tracing to produce 3D models. When the users observes some inconsistencies between the extracted contour and the contour of the structure of interest, they can modify the exported contours using the volume rendering environment making this 3D segmentation model a semi-automatic approach.

5. Summary and Discussion

Through this work, it is shown that the proposed model of denoising across the volume of the data using the refined nonlinear diffusion and determining a threshold for 3D segmentation by entropic maximization based on the spatial and gray-level correlation across the volume help the contour detection by a Canny edge detector; leading to detection of connected contours when possible. This work can be improved by implementing the Canny edge detector in 3D across the volume of image data to further incorporate data from across the serial image sections when detecting contours. The localized contours can be labeled by associated matrices of the coordinates of their sequential pixels making it possible to modify these lists to combine contours when needed and to export the lists to a volume rendering environment for subsequent contour refinement and surface rendering of 3D models.

6. References

1. Bazan, C., and Blomgren, P., Image smoothing and edge detection by nonlinear diffusion and bilateral filter, *Research Report CSRCR 2007*, San Diego State University, San Diego, **2**,1 (2007).

2. Bazan, C., Miller, and M., Blomgren, P., Structure enhancement diffusion and contour extraction for electron tomography of mitochondria, *Journal of Structural Biology*, **166(2)**, 144-155 (2009).

3. Canny, A. A computational approach to edge detection, *IEEE Transactions on Pattern Analysis and Machine Intelligence*, **8**, 679-698 (1986).

4. CATT´E, F., Lions, P.L., Morel, J.M., and Coll, T. Image selective smoothing and edge detection by nonlinear diffusion, *SIAM Journal of Numerical Analysis*, **29(1)**, 182-193 (1992).

5. Gilber, P.F.C., The reconstruction of a three-dimensional structure from projectiosn and its application to electron microscopy. II. Direct methods, *Proceeding of Royal Society of London Series B Biological Sciences*, **182**, 89-102 (1972).

6. Kremer, J.R., Mastronarde, D.N., and McIntosh, J.R., Computer visualization of three-dimensional image data using IMOD, *Journal of Structural Biology*, **116**, 71-76 (1996).

7. Kovesi, P., Edges are not just steps, *Proceedings of ACCV 2002*, The Fifth Asian Conference on Computer Vision, Melbourne, 822-827 (2002).

8. Luther, P.K., Lawrence, M.C. and Crowther, R.A., A method for monitoring the collapse of plastic sections as a function of electron dose, *Ultramicroscopy*, **24**, 7-18 (1988).

9. Perona, P., and Malik J., Scale space and edge detection using anisotropic diffusion, *IEEE Transactions on Pattern analysis and Machine Intelligence*, **12(7)**, 629-639 (1990).

10. Wirjadi, O., Survey on 3D image segmentation, *Technical report*, Fraunhofer ITWN, Kaiserslautern (2007).

11. Xiao, Y., Cao, Z., and Zhang, T., Entropic thresholding based on gray-level spatial correlation histogram, *International Conference on Pattern Recognition 2008*, 1-4 (2008).

7. Acknowledgements

The author thanks Dr Steven Barlow for his help with preparation of samples for electron microscopy. The support of SDSU Electron Microscopy Facility is highly appreciated in producing the microscopic data. The author thanks IMOD Research Group, Dr Peter Kovesi, Dr Tomasi and Dr Manduchi for the open source codes that were partly used in implementation of this model.